

Efficient aberrations pre-compensation and wavefront correction with a deformable mirror in the middle of a petawatt-class CPA laser system

F. CANOVA,¹ A. FLACCO,¹ L. CANOVA,¹ R. CLADY,¹ J.-P. CHAMBARET,¹ F. PLÉ,² M. PITTMAN,² T.A. PLANCHON,³ M. SILVA,⁴ R. BENOCCI,⁴ G. LUCCHINI,⁴ D. BATANI,⁴ E. LAVERGNE,⁵ G. DOVILLAIRE,⁵ AND X. LEVEQC⁵

¹Laboratoire d'Optique Appliquée, ENSTA-Ecole Polytechnique-CNRS UMR 7639, Chemin de la Hunière, Palaiseau CEDEX, France

²Laboratoire d'interaction du rayonnement X avec la matière (LIXAM), UMR 8624, Orsay, France

³Colorado School of Mines, Department of Physics, Golden, Colorado

⁴Dipartimento di Fisica G. Occhialini, Università Milano-Bicocca, Milano, Italy

⁵Imagine Optic, Orsay, France

(RECEIVED 21 March 2007; ACCEPTED 6 October 2007)

Abstract

In this paper, we describe the experimental validation of the technique of correction of wavefront aberration in the middle of the laser amplifying chain. This technique allows the correction of the aberrations from the first part of the laser system, and the pre-compensation of the aberrations built in the second part. This approach will allow an effective aberration management in the laser chain, to protect the optical surfaces and optimize performances, and is the only possible approach for multi-petawatt laser system from the technical and economical point of view. This approach is now possible after the introduction of new deformable mirrors with lower static aberrations and higher dynamic than the standard devices.

Keywords: Adaptive optics; CPA; Femtosecond lasers; Laser-matter interaction; Wavefront distortion

1. INTRODUCTION

Chirped pulse amplification (CPA) (Strickland & Mourou, 1985) has paved the way for high power femtosecond lasers. These laser systems in turn have opened an exciting new research field experimentally, as well as for theoretical studies (Anwar *et al.*, 2006; Danson *et al.*, 2005; Fisher *et al.*, 2006; Flippo *et al.*, 2007; Fuerbach *et al.*, 2005; Kalashnikov *et al.*, 2007; Neumayer *et al.*, 2005; Osvay *et al.*, 2005; Ozaki *et al.*, 2006; Petrov, 2005; Wu *et al.*, 2005). Wavefront correction in high intensity laser chains is a bottleneck on the way to highest intensities (Cowan *et al.*, 1999; Gauthier *et al.*, 1999). The actual trend of laser facilities is to move to increasingly powerful systems, up to the tenth of petawatt. These new systems have more amplification stages, larger beam sizes and complicated CPA schemes, and introduce hundreds of optical surfaces

on the beam path. Wavefront correction of the laser beam is of fundamental importance in modern high intensity laser for two reasons: to optimize the experimental focal spot, so to obtain the maximum intensity for laser-matter interaction, and to address the problem of damage of optical components by spatial modulations and hot-spots. Recent works (Planchon *et al.*, 2005; Bahk *et al.*, 2004; Danson *et al.*, 2005; Neumayer *et al.*, 2005) demonstrated that it is possible, by using a deformable mirror to correct aberrations at the end of the amplification chain, to obtain an improvement of the Strehl ratio up to 90%. The problem of damage of optical components by spatial modulations and hot spot, especially in CPA laser chain, is usually underestimated, due to the difficulty of correlating the damages induced on the optical surfaces to the beam modulations.

A new approach to the problem of damage in CPA laser chain, based on the analysis of temporal and spatial modulations of the stretched beam (Canova *et al.*, 2005), enhances the importance of the evolution of the static aberrations of the deformable mirror, responsible for hot spots formation. The first “classical” solution, to protect the elements in the laser

Address correspondence and reprint requests to: Federico Canova, Laboratoire d'Optique Appliquée, ENSTA-Ecole Polytechnique-CNRS UMR 7639, Chemin de la Hunière, 91761 Palaiseau CEDEX, France. E-mail: federico.canova@ensta.fr

system and to optimize the wavefront, is to filter the aberrations with spatial filters (mainly under vacuum), and relay image all the optical surfaces. This solution induce a huge loss of energy (up to 30% in a spatial filter) and introduces a very complicated optical systems (relay image configuration introduce the danger of ghost foci, for example). The other classical solution is to introduce the deformable mirror at the end of the laser chain. This solution optimizes the focal spot but can't protect the final optics, crystals and diffraction grating. The "AO (adaptive optics) inside" solution guarantees to solve this problem by a change of paradigm.

In the first part of the article, we demonstrate, in an analytical way, the interest of pre-compensation in order to minimize the absolute value of the aberration that builds up in the typical laser amplification chain. Then, in the second part, we define the characteristics that a deformable mirror must have to be used in this configuration, and we show some preliminary characterization of the MIRA0 (from Imagine Optics company, Orsay, France) deformable mirror to validate the performances. Finally, in the third part, we show experimental results of the implementation of this configuration on CPA terawatt laser system (100 fs, 80 mJ) to confirm the efficiency of this approach.

2. A NEW ABERRATIONS CORRECTION PARADIGM: THE MINIMIZATION OF THE ABSOLUTE ABERRATION

The usual aberration correction technique is based on a close loop approach with the deformable mirror at the end of the laser chain, just before the final focusing optics (Fig. 1).

This technique is well established in the literature and can offer excellent results from the point of view of the Strehl ratio optimization (Planchon *et al.*, 2003); however, such an approach to aberration correction, closing the loop at the end of the laser chain, has two major drawbacks, both from a technological and an economical point of view: (1) The size of the deformable mirror is scaled with the laser energy, due to the damage threshold of the optical elements

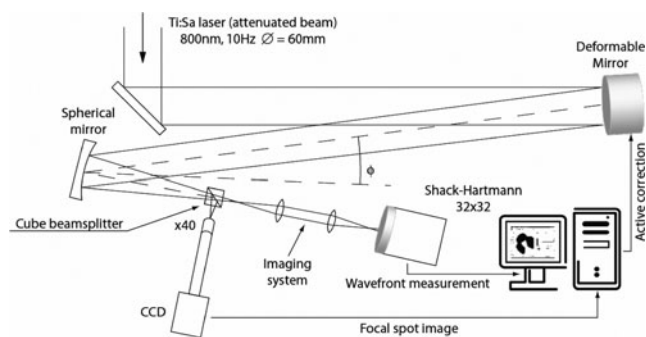


Fig. 1. Typical scheme of close loop aberrations correction, with a deformable mirror. The deformable mirror is placed before the final focusing optic (the experimental optic) and the wavefront sensor is placed after the focal spot.

and coatings, and the price of the device increase correspondingly. (2) The deformable mirror, installed at the end of the amplifying chain, corrects the beam after the full propagation of the aberrations. Aberrations build up while the beam passes through the amplification stages and the effects of the deformations increase linearly with the distance. Therefore, at the end of all of the propagation lines, one has to correct for all the defects that the beam wavefront has accumulated.

These two drawbacks of the present wavefront correction technique open the way to a new approach: instead of compensating the defects at the end, where the size of the beam is large (tens of centimeters in petawatt lasers), and the amplitude of the modulations are maximum (Fig. 2a), we propose to place the deformable mirror and compensate the aberrations in the middle of the CPA laser chain. This solution allows to compensate the aberrations due to the part of the chain before the mirror, and to pre-compensate the aberrations that will build up in the last part of the laser. Choosing this solution allows using a small mirror while minimizing the absolute aberration (Fig. 2b).

The absolute value of the aberrations in Figures 2a and 2b is the same, but in the first case, the mirror should compensate them with the full dynamics, while in the second case, the corrected part and the pre-corrected part relax the constraints in the mirror deformation.

The high spatial frequencies are a special problem, as calculated in Planchon *et al.* (2005), because the deformable mirror can't correct them. In Figure 2, the configuration (a) represents "classical configuration" with the DM at the end of the laser path and filtering stages to cut the high frequency modulations, with large pinholes to reduce the energy loss. A configuration with spatial filter cutting even the low frequency is possible, but the energy loss are high (in the example of Salle Jaune 100 TW laser at Laboratoire d'Optique Appliquée, France, the beam energy goes down

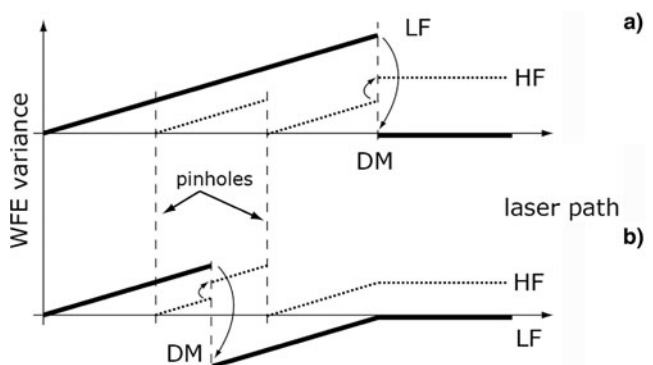


Fig. 2. Graphs showing the effects of the correction of the aberrations at two different place of the amplifying laser chain ((a) representing the correction at the end, and (b) the correction in the middle). This scheme represents the evolution of the high spatial frequencies and the low spatial frequencies of the beam front. WFE represents the wavefront envelope, "pinholes" represent the spatial filtering, installed between the amplifying stages in a CPA laser chain, LF and HF represent the low and the high spatial frequencies, and DM the position of the deformable mirror on the laser path.

from 2 mJ to 0.5 mJ for the first filter, on a 3 mm beam, and from 200 mJ to 150 mJ for the second filter, on a 10 mm beam).

In Figure 2, the configuration (b) represents the effects of the proposed configuration with the deformable mirror on the laser path: the spatial filters, used to eliminate the high frequency modulations, are optional, and depend on the static aberrations of the deformable mirror. In any case, in the configuration (b), to eliminate high frequency modulations we need large filters, with a reduced energy loss.

In the near future, petawatt CPA laser systems will use tight focusing optics to obtain higher intensity on the target and reach new physical regimes, and this kind of optics may introduce a large amount of aberrations (Bahk *et al.*, 2004; in this case, our approach will allow for the use of an additional deformable mirror, at the end of the laser chain, compensating for the aberrations of the focusing optics directly on the target). The advantage of this setup is the possibility to compensate the aberrations before the target with two different mirrors, one for the laser chain and another for the focusing optics. This approach is already used on laser chains as laser megajoule (LMJ) project in France; however it has never been implemented with relatively small and high repetition rate Ti:Sapphire CPA laser chains.

To be realistically, considered as a device able to work in a high intensity environment, typical of a CPA laser chains, the deformable mirror needs to prove special performances and characteristics. The two most important are: (1) Low phase residues; (2) High damage threshold for the mirror membrane.

The phase residues from the deformable mirror introduce high frequency modulations after compensation, and are usually due to membrane imperfections and to the presence of the edges of the actuators (the mirror “footprint”). These modulations are usually independent from the correction induced by the mirror and may induce deep modulations in the reflected beam after some meters of propagation. Such modulations must be low enough, not to become hot spots, which could damage and destroy the most delicate optics (Canova *et al.*, 2005), including the diffraction gratings. Therefore, the modulations amplitude is fundamental for the choice of the best device for this configuration, and represents, as it is specified later, the optimal variable (parameter) to judge the performances of the candidate deformable mirrors. On the other side, the damage threshold for a deformable mirror membrane is an issue depending on a trade-off between efficiency and energy: the final position of the mirror inside the laser chain is defined by the need of a complete illumination of the active surface of the device, necessary to maximize the correction effect, and the maximum fluency that the system can bear without melting.

To validate the feasibility of this new approach, it is necessary to estimate: (1) The modulations due to the static phase aberrations of the mirror, that became amplitude modulations out of the Rayleigh zone of the beam; (2) The evolution of these modulations, when the deformable

mirror attempts to correct some optical distortions (which corresponds to introducing low frequencies deformations of the phase front).

We used a laser propagation code (MIRO CODE, from commissariat à l'énergie atomique (CEAO) (Morice, 2003)) to simulate beam propagation after the deformable mirrors (i.e., after introducing the mirror static aberrations). This code simulates the laser beam propagation solving the Kirchhoff-Fresnel integral at each considered plane. The idea is to define a simulation environment that has the same characteristics of a petawatt laser system. This was used as a benchmark to test the performances of the MIRAO deformable mirror as compared to a more classical bimorph 31 actuators (BIM31) deformable mirror (Planchon *et al.*, 2003). After the validation of the performances we used these simulations to test the pre-compensation configuration.

2.1. Propagation of the phase residues

The residual wavefront introduced by deformable mirrors were recorded with a Shack-Hartmann wavefront sensor (HASO, Imagine Optics, Orsay, France). Such phase residues were then introduced as a phase perturbation at the beginning of the laser chain in the MIRAO simulation. The simulation is a replica of the typical petawatt CPA amplifying chain: the equivalent length, 36 m, is maintained, as well as all the surfaces and the different materials, including the beam resizing during the propagation. Amplification effects are excluded from this first work, because taking them into account would slow down the simulation drastically without any further improvement in the understanding of the phase residue effect. After the propagation of the beam through the whole laser chain, the simulated beam profile shows about 40% peak-to valley (PV) modulation for BIM31 and less than 10% modulations for the MIRAO (Fig. 3). These data show that the amplitude of the modulations induced by the MIRAO deformable mirror, after 36 m of propagation, are small enough to allow the pre-compensation of the aberrations without a major danger for the following optics, especially for the diffraction gratings of the compressor.

2.2. Effects of pre-compensation

The second part of the simulation consisted in testing the effect of pre-compensation on the phase residue. Therefore, we introduced a deep deformation of the mirror, pre-correcting a 4λ astigmatism aberration, and studied the phase residues at the final distance (36 m) as before. In this case, the simulation shows that the high frequency modulations due to the static aberrations are the same as in the ideal configuration, where only the residues are propagated (Fig. 4).

3. THE MIRAO DEFORMABLE MIRROR

In the experiment described in this paper, we have used a new deformable mirror called MIRAO produced by Imagine Optics whose specification can be found in Table 1.

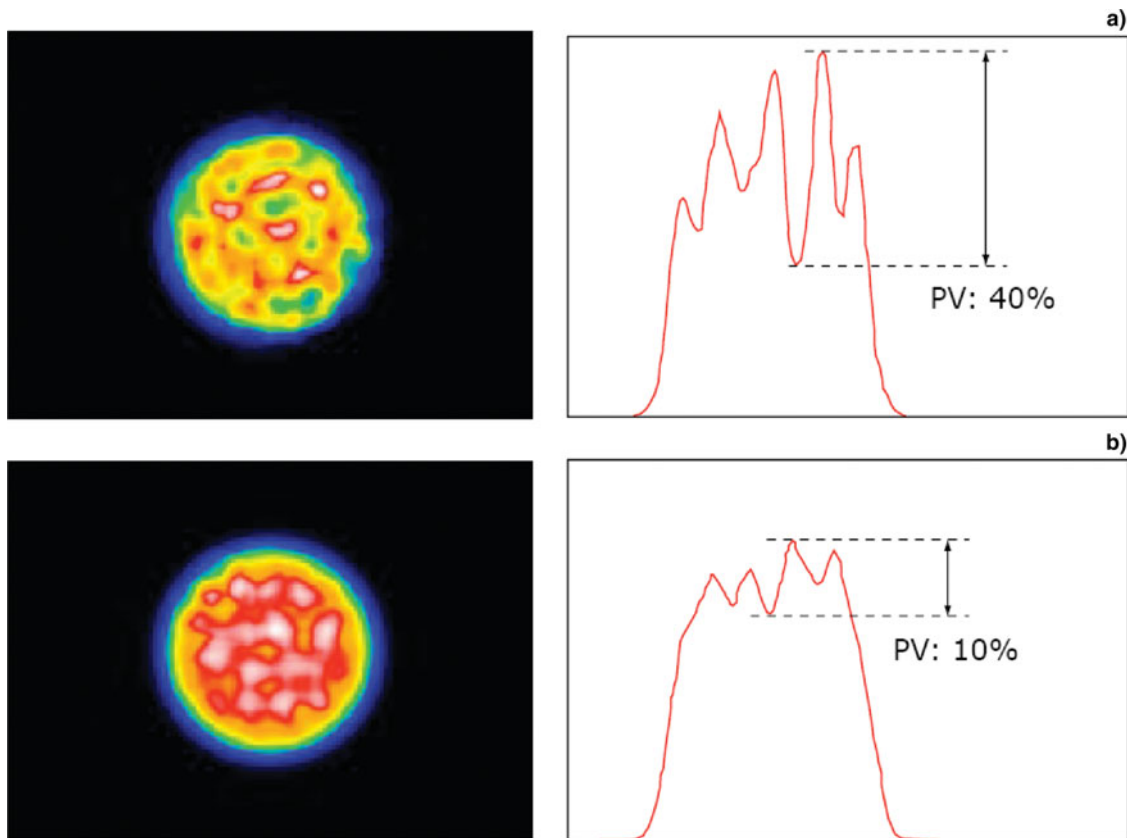


Fig. 3. (Color online) Beam intensity two-dimensional image and profile obtained after the propagation for the phase residues of the MIRA0 and the BIM31 deformable mirrors. The part (a) of this scheme shows the result for the BIM31: the modulation depth about 40%. The part (b) of this scheme shows the result for the MIRA0: the modulation depth is about 10%.

4. EXPERIMENTAL VALIDATION OF THE “AO INSIDE” TECHNIQUE

The technique correcting the aberrations with the adaptive mirror in the middle of the laser chain was tested on a terawatt CPA laser system delivering a recompressed pulse of 80 mJ at 100 fs (Fig. 5). The deformable mirror was placed between the multi-pass amplifiers, where the beam is stretched up to

600 ps, has a diameter of 5 mm, and the energy is 1 mJ. To optimize the spot on the mirror, a double focal system, to up-collimate and down-collimate the diameter, to cover the whole active area, was installed. The Shack-Hartmann wavefront sensor is installed at the output of the compressor. Relay image optics is installed to obtain pupil conjugation between the deformable mirror and the sensor.

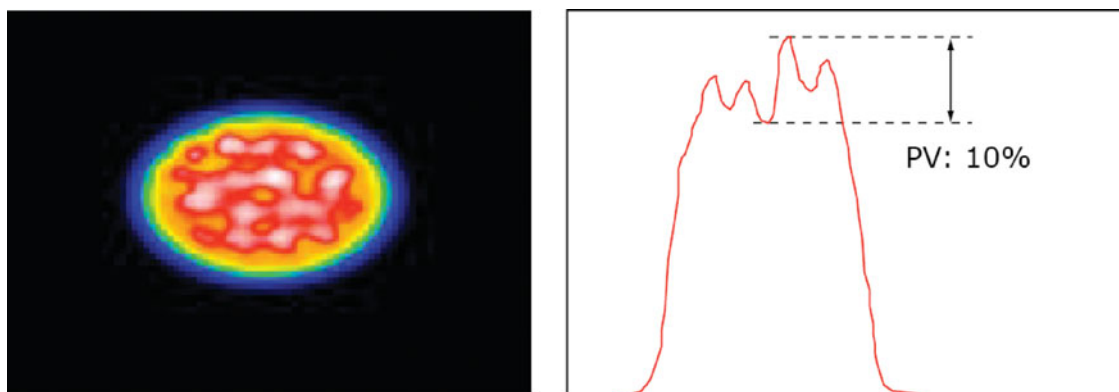


Fig. 4. (Color online) Amplitude profile after propagation of 4λ of astigmatism and of the static aberrations of the MIRA0 deformable mirror. The high frequency modulations due to the phase residues have the same amplitude that in the case of the propagation of the phase residues alone. This simulation shows that the amplitude of the modulations due to the static aberrations are independent of the correction. The beam profile is elliptical due to the strong value of astigmatism pre-corrected (4λ).

Table 1. Main characteristics of the MIRA0 deformable mirrors

Characteristic	MIRA0
Deformation tests (low spatial frequencies)	$\pm 50 \mu\text{m}$
WFE residuals (25% of dynamic)	15 nm
Size of the useful aperture	15 mm
Number of actuators	52
Surface coating damage threshold	measured 1 J/cm^2 at 100 fs estimated 100 J/cm^2 at 1 ns
Membrane CW melting threshold	10 W

4.1. Pupil conjugation and close loop action

Commonly, there is no relay image between the amplifiers in femtosecond CPA laser systems (Pittman *et al.*, 2002). The pupil conjugation between the deformable mirror and the Shack-Hartmann wavefront sensor needs special attention because the thermal lensing in the amplifiers changes the position of the conjugation plane after each multipass. Once the Ti:Sapphire crystals are thermalized, the conjugation plane can be defined for the working conditions of the laser, but each pump configuration (no pumped amplifiers, just one amplifier pumped, both amplifiers pumped), we need to realign the system. We estimated the thermal lens from a simple thermal load model and we compare the predictions with the wavefront sensor measures (Table 2) (Chenais *et al.*, 2003).

Table 2. Ti:Sapphire crystals thermal lens was measured experimentally with the Shack-Hartmann wavefront sensor and estimated from an analytical equation. Pump Power represents the thermal load on the crystals

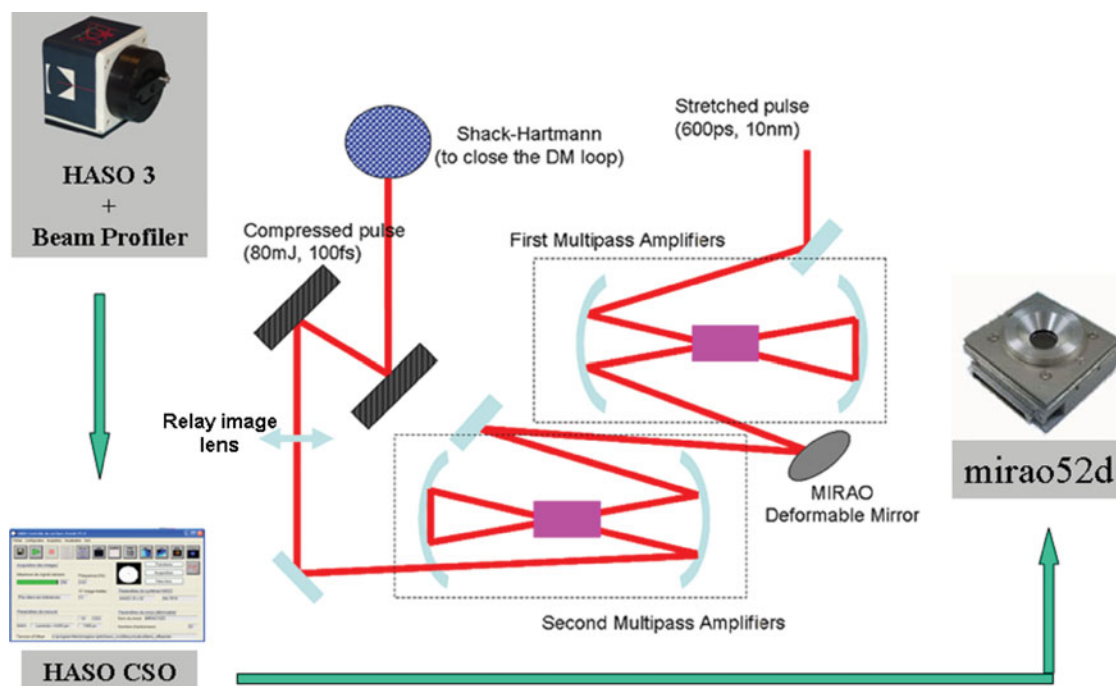
Ti:Sapphire thermal lens	Pump power	Estimated (Shack-Hartmann)	Calculated
First amplifier	0.7 W	62 m	53 m
Second amplifier	4 W	10 m	12 m

Table 3. Experimental results of the wavefront correction

Configuration: oscillator only	RMS / PV	SR
– non corrected	62 nm / 294 nm	0.66
– corrected	23 nm / 108 nm	0.91
Configuration: First amplifier only		
– non corrected	69 nm / 287 nm	0.60
– corrected	23 nm / 108 nm	0.89
Configuration: First and Second amplifiers		
– non corrected	58 nm / 213 nm	0.51
– corrected	29 nm / 149 nm	0.89

4.2. Result of the close loop correction

The close loop system was used to correct the wavefront and optimize the focal spot in three-main configurations. (1) Static aberration correction: the oscillator beam pass

**Fig. 5.** (Color online) Experimental setup used to test the “AO inside” approach. The deformable mirror is between the two multipass amplifiers and the close loop is guarantee by a Shack-Hartman sensor and a wavefront correction algorithm (HASO and CSO, Imagine Optic).

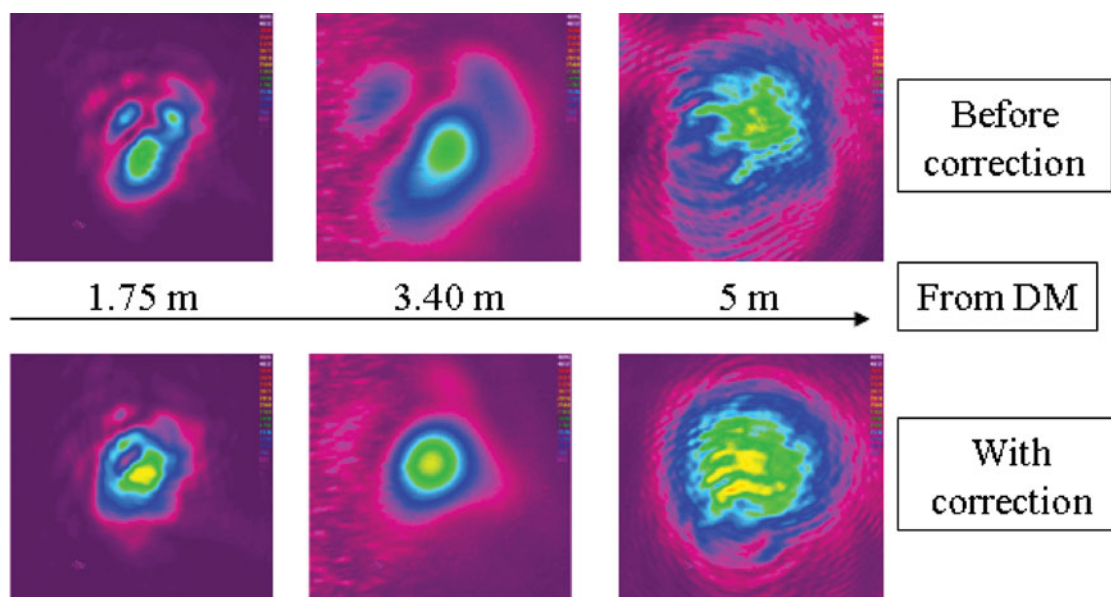


Fig. 6. (Color online) Profile of the propagating beam with and without the DM correction. The profiles show that the spatial modulations induced by the static aberrations are small.

through all of the system, and the multi-pass amplifier are not pumped; (2) The first amplifier pumped: the beam is amplified from a few nJ to 1 mJ and pass through a passive second amplifier; (3). First and second amplifiers pumped: the system is full power and the second stage amplify the beam from 1 mJ to 80 mJ. In all of the three experimental conditions, we were able to correct the aberration and enhance the far-field intensity, and to obtain an improvement in the Strehl ratio (Table 3).

The main objection to this technique was the danger of spatial modulations dues to the high frequencies (HF). The experimental profile measures at different distances with and without the mirror (and with or without corrections) show that the near field profile is not modulated by the mirror footprint (Fig. 6). Observing the spatial profiles, we recognize an increase in the energy in the central Gaussian part of the beam. This effect was confirmed by extraction efficiency: in the unsaturated multi-pass amplifier (the second amplifier), the extraction efficiency increased by 10% once the wavefront was corrected. The pre-compensation approach showed that we were able to introduce 3λ of astigmatism with no arm for the system.

5. CONCLUSIONS

In this paper, we demonstrated the feasibility of the wavefront correction approach based on the installation of the deformable mirror in the middle of the laser chain. Numerical simulations helped us to develop a benchmark to identify the necessary performances of the candidate mirror. The “AO inside” concept has been validated in CPA amplifiers, with excellent performance from the point of view of the Strehl ratio and with no harm to the optics or the diffraction

gratings. Unexpectedly the intermediary field shows an increased amount of energy in the central part of the beam, confirmed by the increase of extracted energy in the unsaturated amplifier. The technique of wavefront correction is validated to be as performing any other technique from the Strehl ratio point of view, and is less expensive and more robust from the laser engineering point of view.

REFERENCES

- ANWAR, M.S., LATIF, A., IQBAL, M., RAFIQUE, M.S., KHALEEQ-UR-RAHMAN, M. & SIDDIQUE, S. (2006). Theoretical model for heat conduction in metals during interaction with ultra short laser pulse. *Laser Part. Beams* **24**, 347–353.
- BAHK, S.-W., ROUSSEAU, P., PLANCHON, T.A., CHVYKOV, V., KALINTCHENKO, G., MAKSIMCHUK, A. & MOUROU, G. (2004). Generation and characterization of the highest laser intensities (10^{22} W/cm²). *Opt. Lett.* **29**, 2837.
- CANOVA, F., CHAMBARET, J.-P., MOUROU, G., UTEZA, O., DELAPORTE, P., ITINA, T., NATOLI, J.-Y., COMMANDRE, M. & AMRA, C. (2005). Complete characterization of damage threshold in titanium doped sapphire crystals with nanosecond, picosecond, and femtosecond laser pulses. *Proc. SPIE* **5991**, 599123.
- CHENAIS, S., DRUON, F., BALEMBOIS, F., LUCAS-LECLIN, G., FICHOT, Y., GEORGES, P., GAUME, R., VIANA, B., AKA, G.P. & VIVIEN, D. (2003). Thermal lensing measurements in diode-pumped Yb-doped GdCOB, YCOB, YSO, YAG and KGW. *Opt. Mat.* **22**, 129–137.
- COWAN, T.E., PERRY, M.D., KEY, M.H., DITMIRE, T.R., HATCHETT, S.P., HENRY, E.A., MOODY, J.D., MORAN, M.J., PENNINGTON, D.M., PHILLIPS, T.W., SANGSTER, T.C., SEFCIK, J.A., SINGH, M.S., SNAVELY, R.A., STOYER, M.A., WILKS, S.C., YOUNG, P.E., TAKAHASHI, Y., DONG, B., FOUNTAIN, W., PARNELL, T., JOHNSON, J., HUNT, A.W. & KÜHL, T. (1999). High energy electrons,

- nuclear phenomena and heating in petawatt laser-solid experiments. *Laser Part. Beams* **17**, 773–783.
- DANSON, C.N., BRUMMITT, P.A., CLARKE, R.J., COLLIER, J.L., FELL, B., FRACKIEWICZ, A.J., HAWKES, S., HERNANDEZ-GOMEZ, C., HOLLIGAN, P., HUTCHINSON, M.H.R., KIDD, A., LESTER, W.J., MUSGRAVE, I.O., NEELY, D., NEVILLE, D.R., NORREYS, P.A., PEPLER, D.A., REASON, C.J., SHAIKH, W., WINSTONE, T.B., WYATT, R.W.W. & WYBORN, B.E. (2005). Vulcan petawatt: Design, operation and interactions at 5×10^{20} Wcm⁻². *Laser Part. Beams* **23**, 87–93.
- FISHER, D.V., HENIS, Z., ELIEZER, S., & MEYER-TER-VEHN, J. (2006). Core holes, charge disorder, and transition from metallic to plasma properties in ultrashort pulse irradiation of metals. *Laser Part. Beams* **24**, 81–94.
- FLIPPO, K., HEGELICH, B.M., ALBRIGHT, B.J., YIN, L., GAUTIER, D.C., LETZRING, S., SCHOLLMEIER, M., SCHREIBER, J., SCHULZE, R. & FERNANDEZ, J.C. (2007). Laser-driven ion accelerators: Spectral control, monoenergetic ions and new acceleration mechanisms. *Laser Part. Beams* **25**, 3–8.
- FUERBACH, A., FERNANDEZ, A., APOLONSKI, A., FUJI, T. & KRAUSZ, F. (2005). Chirped-pulse oscillators for the generation of high-energy femtosecond laser pulses. *Laser Part. Beams* **23**, 113–116.
- GAUTHIER, J.-C., AMIRANOFF, F., CHENAIS-POPOVICS, C., JAMELOT, G., KOENIG, M., LABAUNE, C., LÉBOUCHER-DALIMIER, E., SAUTERET, C. & MIGUS, A. (1999). LULI activities in the field of high-power laser–matter interaction. *Laser Part. Beams* **17**, 195–208.
- KALASHNIKOV, M., OSVAY, K. & SANDNER, W. (2007). High-power Ti:Sapphire lasers: Temporal contrast and spectral narrowing. *Laser Part. Beams* **25**, 219–223.
- MORICE, O. (2003). MIRO: Complete modeling and software for pulse amplification and propagation in high-power laser systems. *Opt. Engin.* **42**, 1530–1541.
- NEUMAYER, P., BOCK, R., BORNEIS, S., BRAMBRINK, E., BRAND, H., CAIRD, J., CAMPBELL, E.M., GAUL, E., GOETTE, S., HAEFNER, C., HAHN, T., HEUCK, H.M., HOFFMANN, D.H.H., JAVORKOVA, D., KLUGE, H.J., KUEHL, T., KUNZER, S., MERZ, T., ONKELS, E., PERRY, M.D., REEMTS, D., ROTH, M., SAMEK, S., SCHAUMANN, G., SCHRADER, F., SEELIG, W., TAUSCHWITZ, A., THIEL, R., URSESCU, D., WIEWIOR, P., WITTRICK, U. & ZIELBAUER, B. (2005). Status of PHELIX laser and first experiments. *Laser Part. Beams* **23**, 385–389.
- OSVAY, K., CSATARI, M., ROSS, I.N., PERSSON, A. & WAHLSTROM, C.G. (2005). On the temporal contrast of high intensity femtosecond laser pulses. *Laser Part. Beams* **23**, 327–332.
- OZAKI, T., KIEFFER, J.C., TOOTH, R., FOURMAUX, S. & BANDULET, H. (2006). Experimental prospects at the Canadian advanced laser light source facility. *Laser Part. Beams* **24**, 101–106.
- PETROV, Y.V. (2005). Energy exchange between the lattice and electrons in a metal under femtosecond laser irradiation. *Laser Part. Beams* **23**, 283–289.
- PITTMAN, M., FERRÉ, S., ROUSSEAU, J.-P., NOTEBAERT, L., CHAMBARET, J.-P. & CHÉRIAUX, G. (2002). Design and characterization of near-diffraction-limited femtosecond 100-TW 10-Hz high-intensity laser system, *Appl. Phys. B Lasers Opt.* **74**, 529–535.
- PLANCHON, T.A., ROUSSEAU, J.-P., BURGY, F., CHÉRIAUX, G. & CHAMBARET, J.-P. (2005). Adaptive wavefront correction on a 100-TW/10-Hz chirped pulse amplification laser and effect of residual wavefront on beam propagation. *Opt. Commun.* **252**, 222–228.
- PLANCHON, T., MERCÈRE, P., CHÉRIAUX, G. & CHAMBARET, J.-P. (2003). Off-axis aberration compensation of focusing with spherical mirrors using deformable mirrors. *Opt. Commun.* **2164**, 25–31.
- STRICKLAND, D. & MOUROU, G. (1985). Compression of amplified chirped optical pulses. *Opt. Commun.* **56**, 219.
- WU, H.C., SHENG, Z.M., ZHANG, Q.J., CANG, Y. & ZHANG, J. (2005). Controlling ultrashort intense laser pulses by plasma Bragg gratings with ultrahigh damage threshold. *Laser Part. Beams* **23**, 417–421.